REAL–TIME DETECTION OF ANOMALIES FOR ATOMIC CLOCK IN SPACE BY MEANS OF THE GLRT

E. Nunzi, G. Saltanocchi
Dept. of Electronic and of Information Engineering
University of Perugia, Italy
Email: emilia.nunzi@diei.unipg.it

INTRODUCTION

The fast and accurate real-time detection of anomalous behavior of atomic clock is crucial for guaranteeing performance of electronic device where clocks are inserted. In fact, an error of the clock signal compromises the correct activity and the reliability of the system. Although the scientific community has deeply analyzed the statistical behavior of the atomic clock, thus providing accurate statistical models for stable clocks in a lab, techniques used for revealing clock anomalies still need to be characterized and customized for clock working in space. In fact, experimental data obtained by measuring the frequency of clocks on satellites show a non-stationary behavior and some missing data. Thus, classical technique used for identifying the anomalous behavior, which are based on the Allan variance estimate, cannot be applied directly to measured data. It follows the interest for innovative statistical methods that improve performance of detection tools. In this context, since few years the Generalized Likelihood Ratio Test (GLRT) technique has been proposed to the scientific community for revealing anomalous behavior of clock for space applications [1]–[5]. The technique, widely used in many application field for detecting signals in noise, has been customized specifically for revealing a frequency jump and/or frequency variance change from a record of acquired measurements data. The GLRT is a quiet convenient tool to be used in this environment since: it does not require data to be stationary, it can be applied to experimental data also when measurements are missing, it can be used also for the anomaly identification, its algorithm implementation is straightforward thus making simple the hardware prototyping. These properties make the algorithm particularly suitable for the real–time detection of anomalies as reliability constraints of clocks on satellites require [6].

Despite its algorithmic simplicity, the theoretical statistical characterization is quite complex because it relies on several parameters strictly dependent on both the anomalies extent and the employed measurement acquisition system. It follows that the interpretation of the detector outcomes is crucial and requires a careful study of the behavior of the GLRT and of its statistical properties.

In this paper, an applicative example of the GLRT to experimental data acquired from a GPS satellite is deeply analyzed and the interpretation of the detector results is discussed by using also the corresponding statistical characterization based on ad–hoc Monte–Carlo simulations.

In particular, it is emphasized that the False Alarm Probability (PFA) value associated to a GLRT outcome depends only on the threshold γ used in the final decision process and is independent of the signal parameters. On the other hand, the Detection Probability (PD) of the detector result is independent of PFA and it relies on several algorithm and measurements parameters such as the number of available data, N, the absolute value of the parameters jump, the number of anomalous samples, N_a, included in the N available data samples. The relationship between PFA and γ has been recently studied and results are explicitly given and applied to the analyzed example.

Furthermore, the paper points out how to evaluate the PFA and PD value corresponding to a detection event and it proposes the use of the GLRT also for both the identification and the timing location of detected anomaly.

GLRT ALGORITHM

The GLRT detection algorithm proposed for revealing anomalies of atomic clock, aims to detect if the clock is working properly or if its measurements experience changes in the mean or in the dynamic range.

Fig.1 shows a conceptual block scheme of the detection method based on the GLRT technique: N measurement data, $\mathbf{x} = \{x[0], x[1], ..., x[N-1]\}$, are processed by the GLRT detector, $T(\mathbf{x})$, that returns a scalar value. The detector output is compared to a given threshold value, γ, in order to decide which one between two statistical hypotheses is the most likely. For the specific case considered in this context, the null hypothesis, $\mathcal{H}_0$, identifies a working clock and the alternative hypothesis, $\mathcal{H}_1$, recognizes a faulting clock.

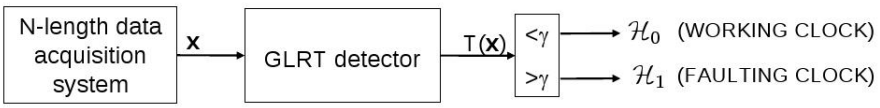

Fig. 1. GLRT block scheme.

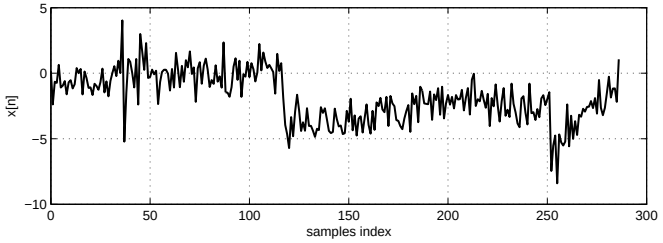

Fig. 2. First order residuals fo data extracted from file mit12674.clk satellite G31 @ 22-4-2004 (Downloaded @ ftp://cddis.gsfc.nasa.gov/pub/gps/products/). An additive offset and a normalization factor have been applied to original data.

Measurement data should respect following constraints: each data sample $x[n]$ can be modeled as a Gaussian random variable and all data samples are independent. The clock is considered to be working if all available data have the same mean and variance values, indicated with μ_0 and σ_0^2, respectively. The clock is considered to be faulting if the mean and/or the variance change their values to μ_1 and/or σ_1^2, respectively, for samples index greater than or equal to an unknown value, n_0.

By following the notation already introduced in [1] and [3], the detector is given by:

$$T(\mathbf{y}) = \log(L_G(\mathbf{y})) = N \log \frac{\hat{\sigma}_{0\_H_0}}{\hat{\sigma}_{1\_H_1}} - \hat{n}_0 \log \frac{\hat{\sigma}_{0\_H_1}}{\hat{\sigma}_{1\_H_1}} \tag{1}$$

where $\hat{\sigma}^2_{0\_H_0}$ is the MLE estimator of σ_0^2 when $\mathcal{H}_0$ is true; $\hat{\sigma}^2_{0\_H_1}$, $\hat{\sigma}^2_{1\_H_1}$ and $\hat{n}_0$ are MLE estimators of σ_0^2, σ_1^2 and n_0, respectively, when $\mathcal{H}_1$ is true.

It should be noticed that the employed measurement data model implicitly assumes that measurement data rate has been normalized to 1 second. Thus, detection performance strongly depend on the relationship between the measurement acquisition rate and the anomaly time–length or, equivalently, on N and n_0, respectively. Moreover, in order to give an appropriate interpretation of the detection results, also the condition $n_0 > N/2$ should be respected, since a detector is conventionally used for revealing anomalies quickly and thus with a number of faulty samples not exceeding the number of "healthy" data.

AN APPLICATION EXAMPLE

Fig.2 shows the behavior of first order phase residuals of GPS satellite G31 on April 22, 2004 that presents an appreciable change in the mean value on sample numbered as 118. Both an offset and a normalization factor have been applied to original data in order to have measurement samples with approximatively zero mean and unity variance just before the large frequency jump.

These data present a clear mean change close to data sample numbered as 118 and this jump is approximatively equal to 4.

The GLRT detector (1) has been firstly applied to the subsequence $\{x[0], x[1], ..., x[99]\}$ of length $N = 100$. Thus, it has been assumed that a real–time measurement bench updates continuously the measurement record and that the GLRT processes subsequences of fixed length $N = 100$ by following a First–In–First–Out (FIFO) strategy. Fig.3 shows the behavior of the GLRT output versus the number of the last acquired sample index. The GLRT has a relatively small value (about 10) for $n \leq 118$, after that, its behavior is continuously increasing thus revealing an anomalous behavior of data. In particular, Fig.3 clearly shows that if the threshold γ is set to 20, the detection is done on sample numbered as 122, i.e. after 5 faulty samples. On the other hand, if γ is too small, thus the comparison process can induce more frequently a false alarm. It follows that the threshold value is strictly related to the PFA and the characterization of the detector is crucial for setting properly the algorithm parameters.

In order to appreciate statistical performance of the detector, the Receiving Operating Characteristic (ROC), i.e. the behavior of the PD versus PFA, is often used. ROCs corresponding to this particular anomaly (i.e. a mean change equal to 4), have

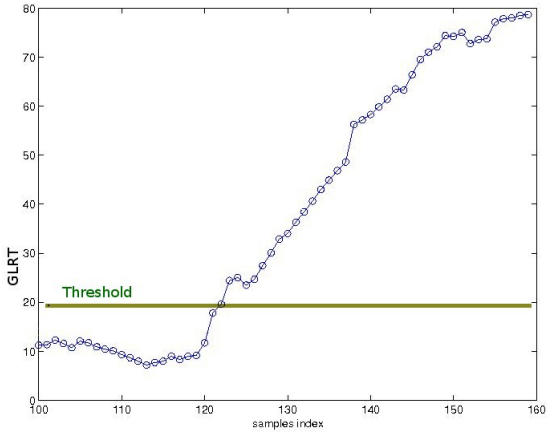

Fig. 3. GLRT output versus the sample index applied to data shown in Fig.2. The GLRT detector processes subsequences each of length N=100 and manages data by following a First–In–First–Out approach.

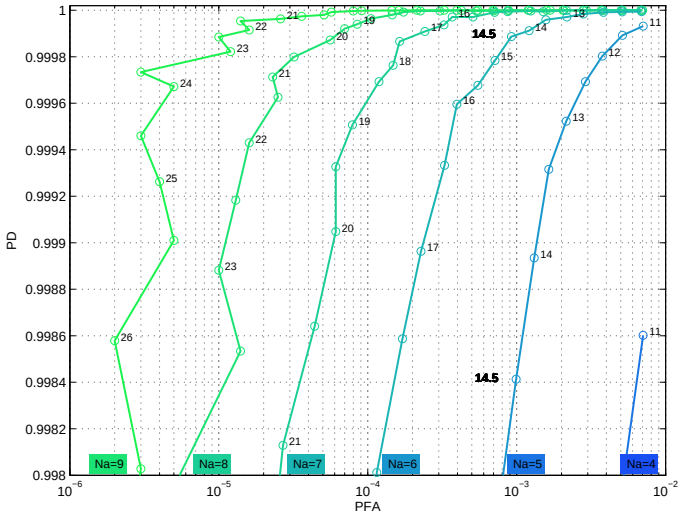

Fig. 4. ROC–Receiver Operating Characteristic for a frequency jump equal to 4 evaluated by means of Monte–Carlo simulations. Each line refers to the indicate number of anomalous samples N_a on $N = 100$ available measurements. Each point has been evaluated by using 2 millions records.

been evaluated by means of intensive Monte–Carlo simulations since a theoretical model is not available yet. In particular, the wide frequency jump considered in this application example, requires the use of a large number (2 millions) of data records, each of length $N = 100$, in order have reliable ROCs. Simulations results are shown in Fig.4

Each line represents the behavior of PD versus PFA for a given number of anomalous samples, N_a, processed by the detector as indicated by the corresponding label. For a given N_a, i.e. for a given curve, a γ value is associated to each couple of coordinates (PFA, PD). Circles in each line emphasize the γ value indicated by the label close to each circle.

In order to explain how to use ROCs in Fig.4 from a practical point of view, let us fix a target maximum PFA value for the detection process, i.e. the $PFA_{max} = 10^{-3}$. Fig.4 shows that $PFA \leq 10^{-3}$ is guaranteed by setting a threshold γ larger than 14.5, that represents the minimum threshold value, γ_{min}, to be set for guaranteeing PFA_{max}. Moreover, it can be deduced that at least 5 anomalous samples are needed. It should be noticed that each value of γ is associated to only one PFA, i.e. all γ values corresponding to a given PFA and labeled in different curves of Fig.4 and are identical.

Once the target PFA_{max} value has been chosen, the minimum number of anomalous samples needed for an accurate detection, which is strictly related to the detection readiness, is fixed by the target PD. In fact, as shown in Fig.4, for a given PFA_{max} (i.e. a given γ_{min}), the PD value increases with N_a. As an example: by requiring $PFA_{max} = 10^{-3}$ and the use of no more than 5 anomalous samples, thus the detector guarantees a $PD = 0.9984$ (i.e. a missed detection probability equal to $1.6 \cdot 10^{-3}$).

If the readiness detection system requirements allows the use of $N_a = 6$ anomalous data, thus, there are two options:

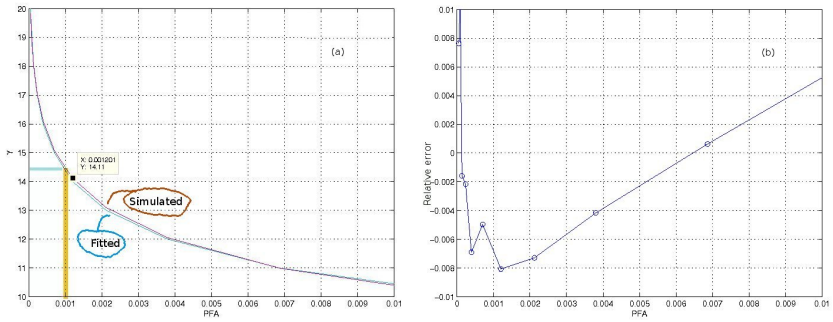

Fig. 5. Behavior of γ versus PFA (a), simulated data on 1 million data record and fitted function as indicated by the corresponding labels. Relative error between simulated and fitted data (b).

1) to keep the threshold value γ to 14.5 (i.e. $PFA = 10^{-3}$) thus obtaining a detector with larger $PD = 0.9998$ (i.e. a smaller missed detection probability equal to $2 \cdot 10^{-4}$);
2) to increase the threshold value γ to a value almost equal to 17.7 (i.e. to reduce the maximum guaranteed PFA to $1.5 \cdot 10^{-4}$) while keeping PD fixed to 0.9984.

It follows that the knowledge of the statistical properties of the GLRT algorithm is fundamental for the practical implementation of the detection process. In this context, in order to evaluate the theoretical relationship between γ and PFA, simulated results shown in Fig.4(a) have been re–arranged as shown in Fig.5 and a least squares fitting algorithm has been applied to all $PFA \leq 10^{-2}$. The following relationship results:

$$\gamma_{FIT} = -1.79 \log\left(\frac{PFA}{3.19}\right) \tag{2}$$

The behavior of γ_{FIT} versus PFA is graphed also in Fig.5(a) (the line close to the label "Fitted") while Fig.5 (b) shows that the error between the fitted and the simulated data is smaller than 1%. Eq.(2) demonstrates that, within the validity range of the fitting process, i.e. for $PFA \leq 10^{-2}$, the threshold γ can be set independently with respect to all algorithm or measurements parameters. For larger PFA values, it has been demonstrated by means of simulations that γ_{FIT} depends on N, i.e. on the observation time–length.

By substituting the value $PFA_{max} = 10^{-3}$ in (2), thus $\gamma_{min} = 14.41$ results, which is coherent with the analysis of the ROC in Fig.4 described before.

GLRT FOR ANOMALY IDENTIFICATION

The GLRT algorithm can be used also for the identification of the anomaly for which it has been designed, since both the anomalies extent and the corresponding timing location is estimated during the detection process. As an example, Figs.6–7 show the behavior of the MLE estimates obtained while computing the GLRT shown in Fig.3 (i.e. applied to experimental data in Fig.2). In particular:

- Fig.6 shows that $\hat{n}_0$ is fixed to the value 118 since the measurement sample indexed as 120. Thus, it can be deduced that the GLRT detects and locates the large anomaly correctly by using just two faulty samples (as confirmed by the visual analysis of data in Fig.2);
- Fig.7 shows that from the sample measurement numbered as 120, i.e. since the anomaly has been detected, the frequency jump (a) and the variance factor (b) are approximatively equal to 4 and 1, respectively.

From these information it can be deduced that an anomaly occurred on the measurement number 118 and that the anomaly is a mean change. Moreover, the anomaly is correctly detected by using 3 faulty samples since the detection is done on the 120–th measurement and the corresponding GLRT outcome is equal to 12. This value, if set as the threshold value, gives a PFA equal to $4 \cdot 10^{-3}$ (see Fig.4 or, equivalently, reverse eq.(2)). Moreover, Fig.4 clearly indicates that by setting $\gamma = 12$ the PD value corresponding to $N_a = 3$ faulty samples is smaller that 0.998 (the exact value is out of the figure). If a PD almost equal to 0.9995 should be assured, thus ROCs states that at least 6 anomalous samples are needed.

It follows that, after the warning signal on the 120–th measurement, a further check should be done, i.e. we have to wait for the acquisition of other three measurement samples and verify the GLRT outcome: if it is increased after each new data sample, thus if the corresponding analysis of estimates confirms the anomaly extent and location (as it happens in Figs.6–7),

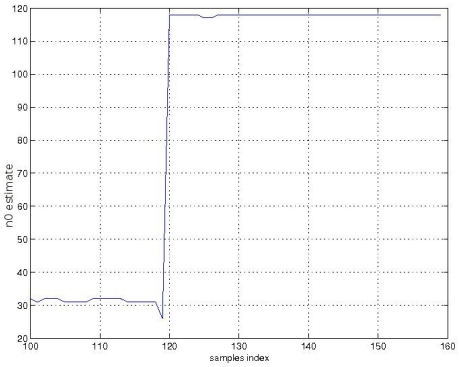

Fig. 6. Behavior of the MLE estimates of the index of the first anomalous data sample versus the index of the last acquired data sample. These estimates have been used for obtaining the GLRT output shown in Fig.3.

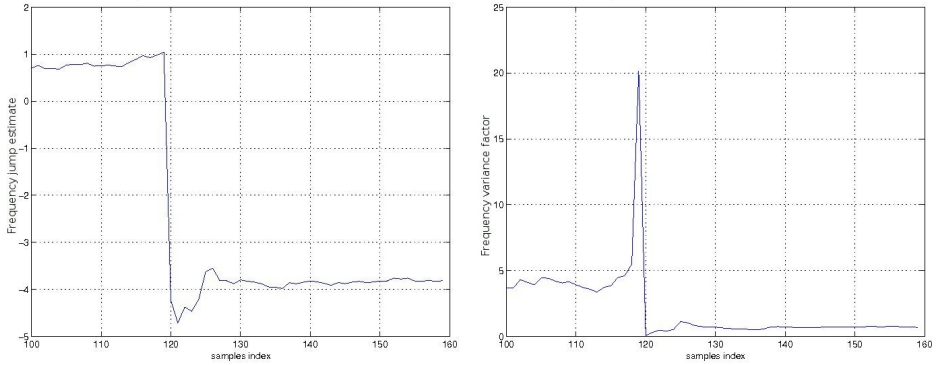

Fig. 7. Behavior of the MLE estimates of the frequency jump (a) and of the variance factor (b) of data shown in Fig.2 versus the index of the last acquired data sample. These estimates have been used for obtaining the GLRT output shown in Fig.3.

thus it can be guaranteed that the detection of an anomaly has been performed with $PFA = 10^{-3}$ and $PD = 0.9995$ (i.e. missed detection probability equal to $5 \cdot 10^{-4}$).

Further considerations follow in order to clarify the interpretation of the GLRT results. Data in Figs.6–7 show that all parameters estimates are stable also before the measurement number 120. In particular, we have $\hat{n}_0$, the frequency jump value and the variance factor almost equal to 31, 0.8 and 4, respectively. These estimates indicate, since the first application of the GLRT, an anomalous behavior from the measurement number 30 and this anomaly could be a frequency jump equal to 0.8 and a change in the frequency variance factor equal to 4. An accurate visual inspection of experimental data in Fig.2 confirm these results. Thus a deeper analysis of the GLRT outcomes is needed. Fig.4 shows that the first GLRT result is almost equal to 11 and subsequent results have a slightly decreasing behavior until the value 8. The non–null GLRT outcome confirms the detection of an anomaly in the first 100 data. By using Eq.(2) it can deduced that if a threshold value equal to 11 is set thus the detection is performed with a $PFA_{max} = 6.8 \cdot 10^{-3}$, however we cannot say anything about the corresponding PD value, neither by analyzing Fig.4. In fact, these ROCs refer to a frequency jump equal to 4 which is not the anomaly estimated in $n = 30$ and statistical characterization experience on similar cases have shown that corresponding PD value is smaller than 40%. Moreover, the GLRT is not applied correctly since the number of anomalous samples is larger than the half of the observed samples. This is demonstrated by the decreasing behavior of the GLRT.

It is clear that a theoretical relationship between PD and the various GLRT parameters (i.e. N_a, N, anomalies extent) is important. The sensitivity of the GLRT to both the frequency jump and variance factor change are currently in progress.

CONCLUSIONS

In this paper an applicative example of the GLRT detector has been presented in order to clarify interpretation of results when it is applied to measurements from atomic clocks. It has been shown that a correct employment of the information estimated in the detection process allows both the identification and the timing–location of the clock faults. Moreover, it has

been emphasized that the a–priori knowledge of the statistical performance of the detector gives criteria for implementing the detection process which is strictly dependent also on the parameters of the employed measurement system.

In particular, results of the research performed in the last year on the analysis of the relationship between the detection threshold value and detector false alarm probability has been explicitly given and applicative examples that show its practical use have been described.

The relationship between detector parameter, anomalies extent, specifics of the measurement system and detection probability is complicated and research on this topic is still in progress.

ACKNOWLEDGMENT

This work has been supported by the Italian Ministry PRIN 2007 program (ARCADIA project).

REFERENCES

[1] E. Nunzi and L. Galleani and P. Tavella and P. Carbone, "Detection of Anomalies in the Behavior of Atomic Clocks," *Instr. and Meas., IEEE Transactions on*, pp. 523–528, Apr. 2007.

[2] E. Nunzi and P. Carbone and P. Tavella, "Fault detection in atomic clock frequency standards affected by mean and variance changes and by an additive periodic component: the GLRT approach," *Instr. and Meas. Tech. Conf.*, May 2008.

[3] E. Nunzi, P. Carbone, *Monitoring Signal Integrity of Atomic Clocks by Means of the GLRT*, Metrologia, 45 (2008), S103-S107.

[4] E. Nunzi, D. D'Ippolito, "A novel theoretical analysis of fault detection for atomic clock," Proc. of the IEEE *AMUEM 2009* Conf., July 2009, Bucharest.

[5] E. Nunzi,G. Barchi, U. Bartoccini, "Methods and tools for frequency jump detection," Proc. of the IEEE *AMUEM 2009* Conf., July 2009, Bucharest.

[6] F. Soualle, T. Beck, H. Trautenberg, D. Felbach, L. Stopfucken, J. Wendel, Francisco Amarillo Fernandez, A Fernndez, M. Snchez Nogales "New Concept for the On-Board Master Clock Generation Unit for Future Galileo Satellites" Proc. *Int. Tech. Meeting of The Institute of Navigation*, San Diego, CA, January 25 - 27, 2010.

[7] S. M. Kay, "Fundamentals of Statistical Signal Processing, Volume 2: Detection Theory," *Prentice Hall*, 1998.

[8] S. M. Kay, "Fundamentals of Statistical Signal Processing, Volume 1: Estimation Theory," *Prentice Hall*, 1998.

[9] David W. Allan, " Time and Frequency (Time Domain) Characterization, Estimation, and Prediction of Precision Clocks and Oscillators," *Ultrasonics, Ferroelectrics, and Frequency Control. IEEE Transactions on*, vol. UFF-34, No 6., Nov. 1987.

[10] IEEE Standard Definitions of Physical Quantities for Fundamental Frequency and Time Metrology. Random Instabilities, IEEE Standard 1139, 1999.

[11] M. Weiss, P. Shome, R. Beard, "GPS signal integrity dependencies on atomic clocks," Proc. *38th Annual Precise Time and Time Interval (PTTI) Meeting*, Washington DC, Dec 2006, pp. 439-448